

*Supporting Information*

**Stress-transfer from polymer substrates to monolayer and few-layer graphenes**

Ch. Androulidakis<sup>1</sup>, D. Sourlantzis<sup>2</sup>, E.N. Koukaras<sup>1,3</sup>, A.C. Manikas<sup>2</sup> and C. Galiotis<sup>1,2\*</sup>

<sup>1</sup>*Institute of Chemical Engineering Sciences, Foundation of Research and Technology-Hellas (FORTH/ICE-HT), Stadiou Street, Platania, Patras, 26504 Greece*

<sup>2</sup>*Department of Chemical Engineering, University of Patras, Patras, 26504 Greece*

<sup>3</sup>*School of Science & Technology, Hellenic Open University, Patras, 26222 Greece*

\*Corresponding author: [c.galiotis@iceht.forth.gr](mailto:c.galiotis@iceht.forth.gr), [galiotis@chemeng.upatras.gr](mailto:galiotis@chemeng.upatras.gr)

## 1. Derivation of equation for estimation of the ISS

In previous works<sup>1, 2</sup> it was shown that the strain transfer profiles obtained by the Raman measurements can be converted into interfacial shear stress profiles along the length of the graphene flake by using continuum theory. Considering the balance of forces at a graphene-polymer interface we can solve for the ISS using equation 1. This relation describes the stress-transfer mechanism from a polymer matrix substrate to a stiff inclusion since the transfer mechanism is shear at the interface which is converted into normal stress at the graphene. Considering an infinitesimal flake of length  $dx$  near its edge, then the balance of stress at the interface is drawn in figure S1 and can be estimated given by the following relation:

$$\frac{d\sigma_x}{dx} = -\frac{\tau_t}{t_g} \Rightarrow \tau_t = -t_g \cdot E_g \cdot \frac{d\epsilon_x}{dx} \quad (1)$$

where  $\tau_t$  is the shear stress at the surface of the flake,  $\sigma_x$  is the axial stress of the flake and  $t_g$  is the thickness of the graphene flake<sup>3, 4</sup> and  $E_g$  is the graphene's Young modulus<sup>5</sup>.

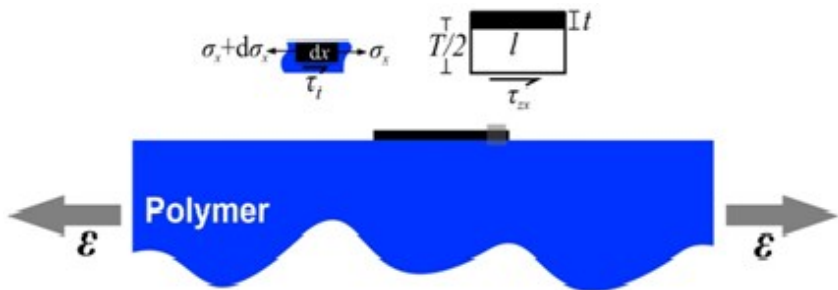


**Figure S1:** Illustration of stress equilibrium in a simply supported graphene flake on a polymeric bar. Axial and shear stresses in representative elements of the flake are also shown. Figure taken from previous work<sup>6</sup>.

## 2. Stress transfer in few-layer-polymer system

### Bilayer

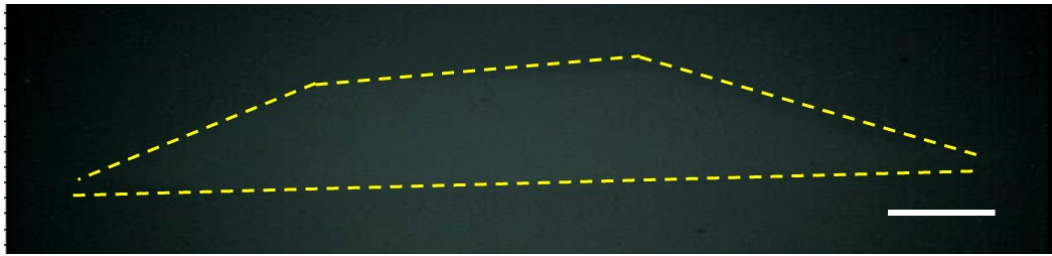


**Figure S2.** Optical image of the second examined bilayer graphene flake. The yellow dotted lines denote the shape of the flake and the geometry of the edges. The scale bar is 10 microns.

We tested another bilayer flake with both edges of angular shape as seen in the following optical image. The situation is quite complex as it seems that up to 0.80% strain there is, in certain cases, a considerable transmission of axial stresses from the edges of the flake with no clear shear transfer mechanism. Beyond that level the strain locks at about 0.2% and 0.6% for the left and right-hand side edges, respectively, and there is some stress built up to 1.50% strain. For these strain levels the transfer lengths are of the order of 20  $\mu\text{m}$  from either side which is approximately twice the values obtained for the square end of monolayer graphene at similar strain (fig. 3b).

For the bilayer shown in figure S2, the shift of the 2D peak is in excellent agreement with the bilayer presented in the main text, with shift rate being  $-44.4 \text{ cm}^{-1}/\%$  (figure S3A). The strain profiles for various levels of tension are presented in figure S3B and in S3C the slopes ( $d\epsilon/dx$ ) are presented for all the tensile strain levels. The slopes are lower than the corresponding ones for the bilayer presented in the main text. We attribute this difference to the angular shape of the edges (in contrast to the square edges presented in the specimens of main text) and to the significant amount of axial transmission through the edges in this case.

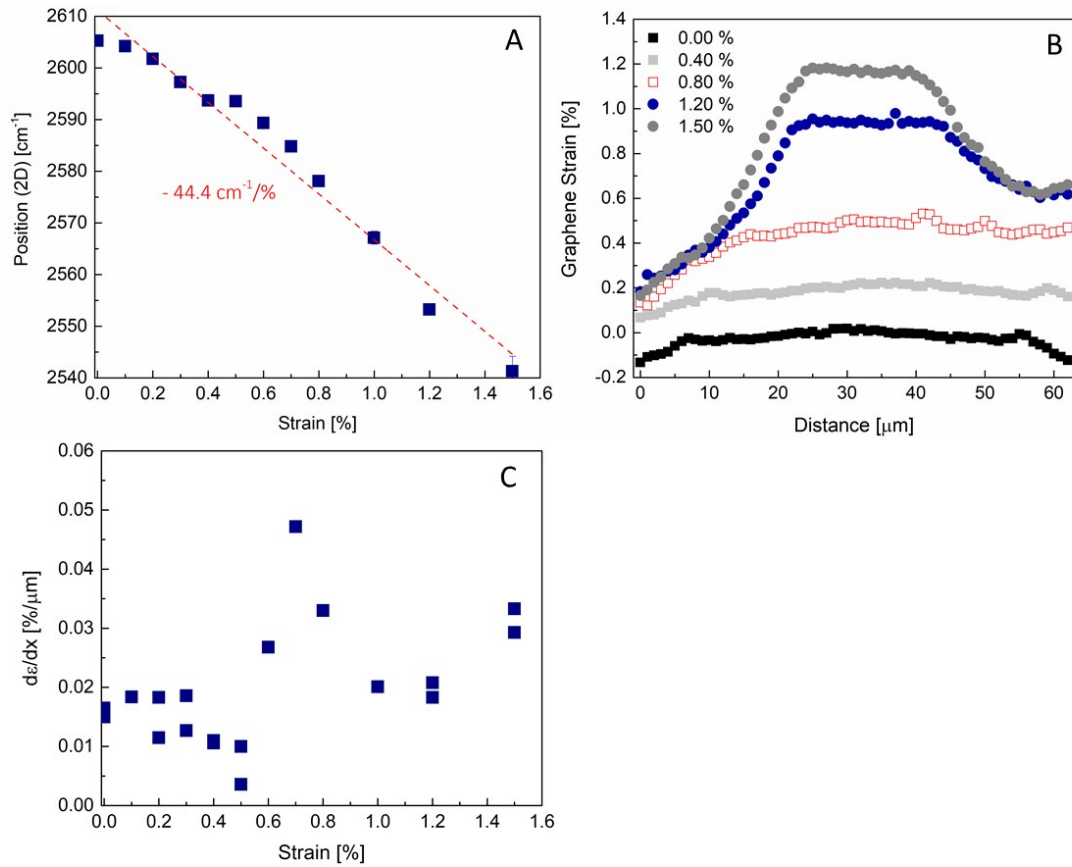


**Figure S3.** A) The shift of the 2D peak for a bilayer graphene with length of  $\sim 62 \mu\text{m}$ . The y-axis represents the actual strain in the graphene based on the shift of the 2D peak and explained in detail in the main text, while the inset values represent the applied strains. B) The strain transfer profiles for selected strain levels.

### Trilayer

We examine and another trilayer with relatively smaller length of  $\sim 28 \mu\text{m}$ . In this case the shift rate of the 2D peak is significantly smaller with value of  $-24.5 \text{ cm}^{-1}/\%$  as seen in figure S4B. We observe initially a strain build-up from the one edge and at the other an axial tensile stress is acting, as observed in the other cases too. The length is small and reaches the transfer length at low strain ( $\sim 0.5\%$ ) resulting further in problematic strain transfer. We note that this shift rate for trilayer has been observed in other studies by us<sup>1</sup> and others<sup>7</sup>. Actually the small length explains the discrepancies for the case of the trilayer where a range for the shift of the 2D peak has been measured. From the shift of the 2D peak is apparent that this trilayer was

stretched only up to  $\sim 0.50\%$  of applied tension to the beam, while the actual strain in the graphene lattice is even smaller as deduced from the shift of the 2D peak.

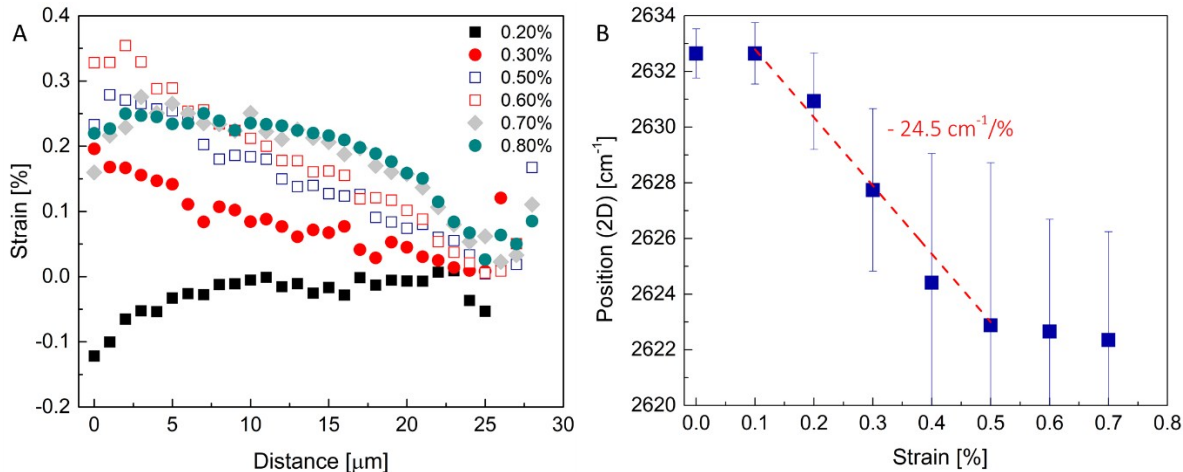


**Figure S4.** A) The shift of the 2D peak for trilayer graphene with length of  $\sim 28 \mu\text{m}$ . The y-axis represents the actual strain in the graphene based on the shift of the 2D peak and explained in detail in the main text, while the inset values represent the applied strains. B) The strain transfer profiles for selected strain levels.

### 3. ISS distribution across the length of the examined flakes for selected levels of strain

#### Single layer

In the following figure the distribution of the ISS across the length of the examined single layer is presented in figure S5 for representative levels of tensile strain. The ISS profiles confirm the increase of transfer length with the increase in tension. Clearly the ISS profiles for the single layer are remarkably smooth and the increasing constant ISS is seen at the edges. The critical length reaches a value of more than twenty microns at high tensile strain  $\sim 1.60\%$  for the a simply supported flake.

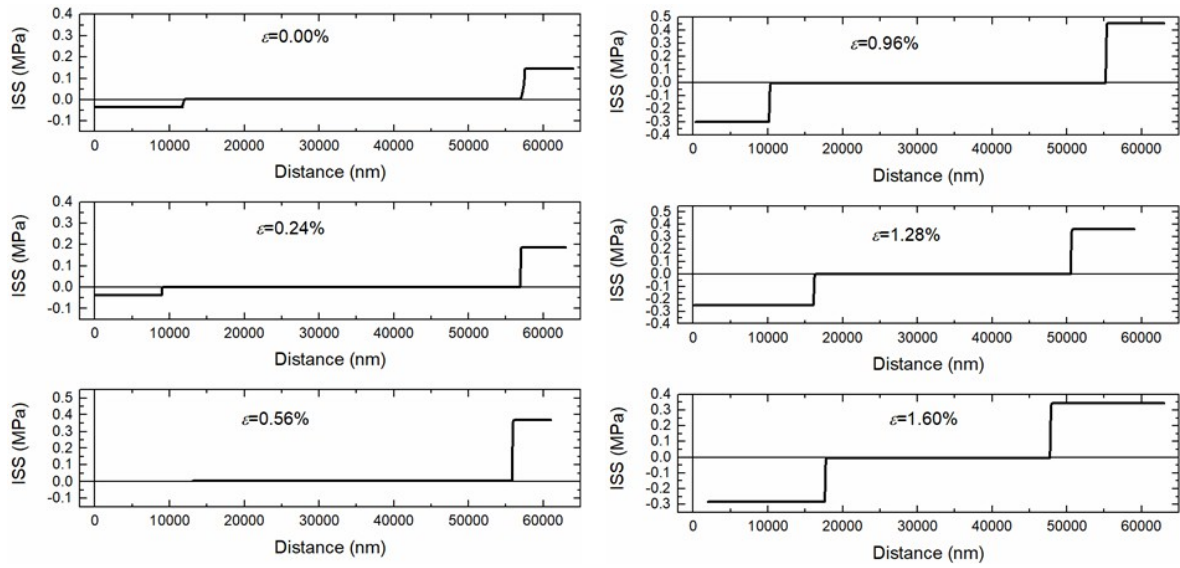


**Figure S5.** The distribution of the ISS across the length of the single layer for representative levels of tension.

#### 4. Structural changes observed by the line-shape of the 2D Raman peak under tension

It has been observed previously that few-layer graphene under tension fully embedded in polymers, lose the stacking order due to relative interlayer changes in the stacking order<sup>8</sup>. This is deduced by the changes in the line-shape of the 2D peak, which becomes symmetric as the load increases, and the sub-peaks of the few-layer are not distinguished<sup>8</sup>. Herein, we observe changes in the line-shape of the 2D peak as seen in figure S6. The change in the shape is apparent, confirming the presence of changes in the stacking of the bilayer and its effect on the strain profiles as discussed in the main text.

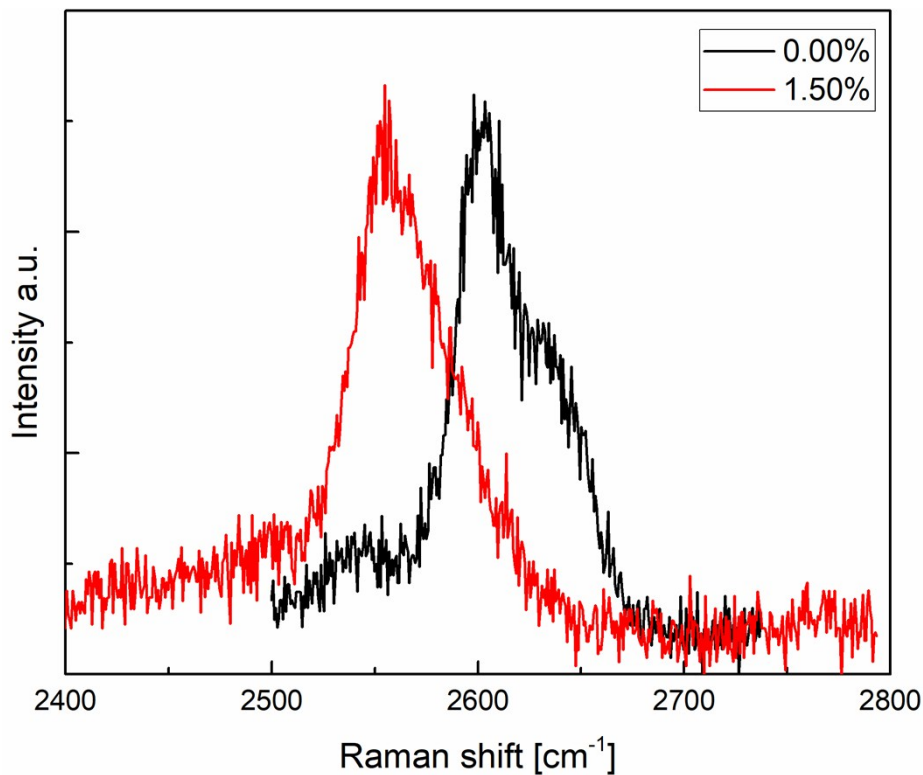


**Figure S6.** The spectra of the 2D peak for the bilayer flake for tension at 0% and 1.50% nominal strain. The change in the shape is apparent, indicating the presence of interlayer changes in the stacking order of the flake.

1. C. Androulidakis, E. N. Koukaras, J. Rahova, K. Sampathkumar, J. Parthenios, K. Papagelis, O. Frank and C. Galiotis, *ACS applied materials & interfaces*, 2017, **9**, 26593-26601.
2. C. Galiotis, *Composites Science and Technology*, 1991, **42**, 125-150.
3. H.-K. Jeong, Y. P. Lee, R. J. W. E. Lahaye, M.-H. Park, K. H. An, I. J. Kim, C.-W. Yang, C. Y. Park, R. S. Ruoff and Y. H. Lee, *Journal of the American Chemical Society*, 2008, **130**, 1362-1366.
4. Y. K. Koh, M.-H. Bae, D. G. Cahill and E. Pop, *Acs Nano*, 2010, **5**, 269-274.
5. C. Lee, X. Wei, J. W. Kysar and J. Hone, *Science*, 2008, **321**, 385-388.
6. G. Anagnostopoulos, C. Androulidakis, E. N. Koukaras, G. Tsoukleri, I. Polyzos, J. Parthenios, K. Papagelis and C. Galiotis, *ACS applied materials & interfaces*, 2015, **7**, 4216-4223.
7. L. Gong, R. J. Young, I. A. Kinloch, I. Riaz, R. Jalil and K. S. Novoselov, *ACS nano*, 2012, **6**, 2086-2095.
8. O. Frank, M. Bouša, I. Riaz, R. Jalil, K. S. Novoselov, G. Tsoukleri, J. Parthenios, L. Kavan, K. Papagelis and C. Galiotis, *Nano letters*, 2011, **12**, 687-693.